Particle Simulations of Radio Wave Scattering by Small Objects covered with a Charged Particle Layer

Miyake, Yohei

Takagi, Junya

Journal of Evolving Space Activities
Vol. 1, Article No. 50, 2023
DOI: 10.57350/jesa.50

Particle Simulations of Radio Wave Scattering by Small Objects covered with a Charged Particle Layer

By Yohei MIYAKE,[1)] and Junya TAKAGI,[1)]

[1)] *Graduate School of System Informatics, Kobe University, Kobe, Japan*

(Received August 30th, 2022)

The present paper addresses the development and demonstration of a numerical approach to study the characteristics of radio wave scattering by a solid object in space covered by a charged particle or plasma layer. The plasma conditions near the surface of the object are totally different from those of a pristine plasma in space, due to various types of ionization processes occurring at the plasma–body interface. This sometimes results in the formation of a dense plasma layer around the surface, which significantly alters the electromagnetic properties of the object. Such processes are relevant to a broad range of in-space radio applications such as radar observations of space debris, meteors, small dust grains, and re-entry objects. This paper proposes a new numerical approach of applying the particle-in-cell simulations to the scattering analysis. PIC is a well-established first-principles model that provides a kinetic description of a plasma by following the trajectories of an ensemble of charged particles in self-consistent electromagnetic fields. It is advantageous to include plasma kinetic effects as well as nonlinear behavior of the plasma in a straightforward manner. A number of numerical techniques such as improved treatments for conducting object surfaces and the field decomposition capability are implemented for the present study. The proposed method is applied to a simple situation of wave scattering from a conducting object covered by a dense electron layer. The simulation reveals an antenna-like behavior of the electron layer swayed by an incident wave, and its contribution to the differentiated wave scattering properties.

Key Words: Electromagnetics, Radio Wave Scattering, Space Plasma, Particle Simulation

Nomenclature

a	:	radius
B	:	magnetic field
c	:	speed of light
e	:	elementary charge
E	:	electric field
I	:	electron current
I_{r0}	:	initially released electron current
J	:	plasma current density
k	:	Boltzmann constant
m	:	particle mass
n_e	:	electron density
$n_{e,sf}$	:	electron density at PEC surface
q	:	charge carried by particle
r	:	particle position
t	:	time
T_e	:	electron temperature
v	:	particle velocity
ε_0	:	permittivity of vacuum
ϵ	:	electron kinetic energy
μ_0	:	permeability of vacuum
ρ	:	charge density
σ_e	:	radar cross section with electron layer
σ_f	:	radar cross section in free space
Φ	:	electric potential
Φ_{PEC}	:	potential of PEC
Superscripts		
i0	:	incident wave
i0	:	field amplitude of incident wave
se	:	scattered field by PEC object
so	:	scattered field by electron layer

1. Introduction

Solid objects placed or moving in space are subject to the formation of non-uniform charged particle (or plasma) layers near their surfaces due to object-plasma interactions as well as various processes such as photo-, secondary, and thermal ionization. These layers potentially alter the electromagnetic scattering properties of the objects. The degree of change is frequency dependent and will be significant near and below plasma resonant frequencies with imposed electromagnetic oscillations. The scattering properties of the objects covered with charged particle layers are of particular interest in the context of in-space radio wave applications (e.g., radar detection of space debris, meteors, small dust grains, and re-entry objects).[1–5)]

The properties of wave scattering by plasma-covered objects have been extensively studied in both theoretical and numerical approaches.[6,7)] Plasma is a dispersive, anisotropic, dissipative, and nonlinear medium, depending on the conditions of applied magnetic field, collisions, temperatures, and the amplitude of applied fields. Previous works have employed different levels of complexity of dielectric representations for a plasma. The characteristics of radio wave transmission and reflection through such a dielectric medium have been studied for a one-dimensional slab model.[8,9)] In higher dimensions, the electromagnetic scattering by cylindrical and spherical objects has been examined using the finite-difference-time-domain (FDTD) simulations, combined with a plasma dielectric model.[10–12)]

The problem-specific plasma modeling and approximations have been applied to the research topic with considerable success. Meanwhile, efforts to develop a self-consistent kinetic plasma model may also be of potential value. Such first-principles plasma modeling has been put to practical use in the study of fundamental plasma processes such as shocks, turbulence, and various nonlinear phenomena. When applied to the radio scattering problems, however, the approach would also have drawbacks. As the kinetic model must resolve a Debye-scale plasma structure for numerical stability, the computational cost of simulating a cold (but finite temperature) plasma is generally high, which prohibits us from assuming realistic physical conditions. Despite this aspect, the development and in-principle verification of the approach is worth pursuing, as some advanced plasma kinetic models would be a promising solution to the open problem.[13)]

In the present study, we employ the particle-in-cell (PIC) model and its in-house implementation called EMSES.[14)] PIC is a well-established first-principles model that provides a kinetic description of a plasma by following the trajectories of an ensemble of charged particles in self-consistent electromagnetic fields.[15)] It is advantageous to include the plasma kinetic effects as well as the nonlinear behavior of the plasma in a straightforward manner. We have developed a number of numerical techniques such as improved treatments for conducting objects as well as a field decomposition technique of incident and scattered fields at an object surface and within a plasma layer.

The remainder of the paper is organized as follows: In Section **2.**, we review the plasma formulation and the additional functions used in the PIC computations. In Section **3.**, the proposed numerical method is demonstrated in its application to two-dimensional simulations of wave scattering processes from a circular object (which is equivalent to a cylinder in three dimensions) covered by a dense electron layer. The discussion and conclusions are then given in Section **4.**.

2. Numerical Modeling

EMSES was originally designed for the study of plasma and electromagnetic processes emerging near solid surfaces. Its basic algorithm for solving a coupled system of particle dynamics and electromagnetics follows the conventional PIC method.[16,17)] The electromagnetic field is represented as Eulerian variables defined discretely on the computational grid points, whereas the plasma is represented as a bunch of charged Lagrangian particles, each representing many real plasma particles, distributed over a computational domain. The computational sequences and field component assignments of EMSES are summarized in Fig. 1. The two sets of governing equations are coupled with each other, through computational phases of the field interpolation and the particle momentum (or current) scattering. These numerical procedures also provide an interconversion algorithm between the Lagrangian (particle) and Eulerian (field) variables. The field and particle variables are then advanced in the time domain by solving the Maxwell's equations, and Newton's equations of motion, respectively, by employing the finite difference scheme.[18–20)] The electromagnetic field components are assigned on a staggered grid based on the Yee scheme.[21)] A charge density and the vector components of a current density are assigned such that the components confirm the finite difference scheme used to update the electromagnetic field.

The functional feature of EMSES is the numerical treatment of solid surfaces in contact with plasma. EMSES is capable

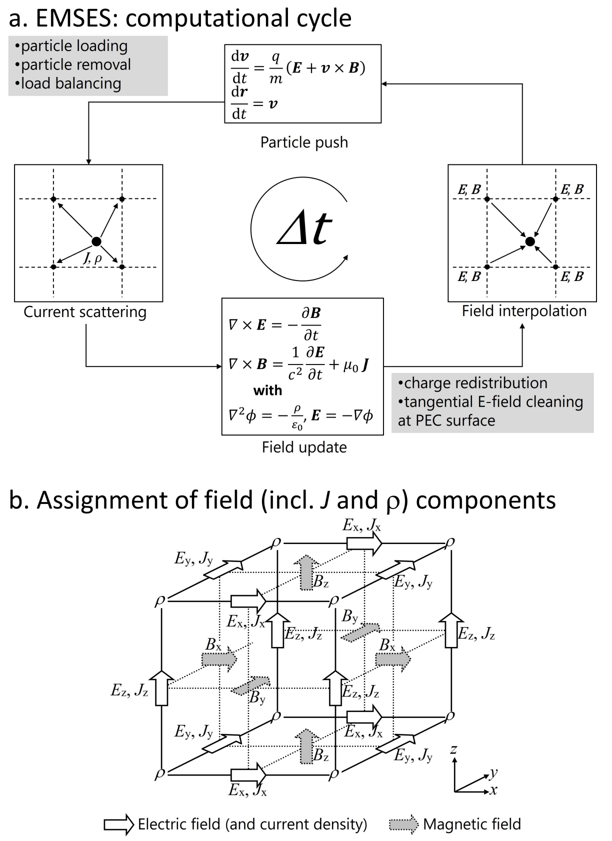

Fig. 1. (a) Computational sequences of EMSES. In each computational cycle, the particle positions and velocities are advanced in time by solving the equations of motion, and the electromagnetic fields are updated by solving Maxwell's equations. The Lorentz field interpolation and plasma current deposition provide an interconversion algorithm between the Lagrangian (particle) and Eulerian (field) variables. A set of procedures for solid surfaces and parallel computation is also included in the cycle. (b) Assignment of field vector components and charge density around a cubic unit cell based on the Yee algorithm.

of incorporating perfectly conducting or insulating structural objects into electromagnetic particle computations. The object surfaces are represented as internal boundaries that satisfy appropriate conditions for both particles and field components. Once a charged particle collides with a solid structure, the particle is regarded as being captured by the surface and is no longer processed as a "free particle". EMSES keeps monitoring particle positions and eliminates captured particles from a list of active particles. Some applications require particle release processes from a surface. In this case, EMSES loads new particles with appropriate positions and velocities according to the physical models considered.

An electric charge carried by a particle colliding with the object is accumulated on its surface. This physical process is implicitly reflected in an (longitudinal) electric field, which is updated based on the Ampère-Maxwell equation. Thus, we do not need any special treatment in a numerical aspect, which is a distinct feature from the standard electrostatic PIC simulations.[22)] The same argument applies to a particle release process. In this case, the electric field is updated so that the surface acquires an opposite charge to that of the released particle.

The Perfect Electric Conductor (PEC) condition is a key factor for high-fidelity reproduction of scattered electromagnetic fields from an object surrounded by a layer of charged particles. At the surface of the PEC, the tangential electric field must be zero at all computational time steps. A requirement that differs essentially from the standard FDTD formulation[19] is that the total field solution should also satisfy an equipotential condition held over the surface of the structure. To satisfy this key requirement, EMSES has a dedicated numerical routine to formulate an electrostatic induction. The routine uses Poisson's equation as an auxiliary solver for an electric potential. Based on potential values obtained at the surface of the structure, the routine redistributes electric charges over the surface so that the new charge distribution produces an equipotential on the PEC surface. Such a charge distribution is obtained from a pre-calculated capacitance matrix,[17] which associates potential values with charge densities at all grid points defined on the PEC. Once the electrostatic field cleaning is complete, a residual electric field on the PEC surface is purely transverse. At this stage, EMSES can correct the transverse field by simply adding an electric field that cancels out the residual tangential field out.

The numerical algorithm outlined above conforms the decomposition analysis of incident and scattered fields. The electric field added to cancel out the residual tangential field serves as a source of a self-propagating wave field. This can be extracted for the detailed analysis of the scattered field by the PEC. The latest version of EMSES is capable of decomposing a total field into an incident field, a field component scattered by the PEC, a field component scattered by charged particle populations, and the electrostatic field.

The PIC method must handle a huge number of Lagrangian particles, corresponding to a total problem size of a few terabytes. Such large-scale problems require high-performance parallel computing. EMSES has been parallelized using the domain decomposition approach. A challenging issue in parallelizing PIC computations is the possible severe computational load imbalance associated with plasma inhomogeneity due to the presence of solid structures. EMSES employs the OhHelp dynamic load-balancing algorithm to cope with this issue and can maintain good scalability for computations using thousands of MPI processes.[23,24]

3. Numerical Simulation

3.1. Simulation setup

The numerical method is demonstrated in its application to a two-dimensional radio wave scattering problem, which comes with a dense electron layer attached to a perfect conductor. The electron density profile is a key component of the investigations. In previous works, the profile is generally treated as one of the predetermined parameters of the simulations.[10–12] However, the density profile is now no longer predetermined, but self-consistently reproduced by solving the particle dynamics. Thus, the numerical analysis consists of two successive simulation phases. The first simulation phase focuses on the processes of electron emission and recollection by a PEC surface to obtain a steady-state solution of an electron density profile. In the second simulation phase, we apply an incident radio wave to the object accompanied by the electron layer and evaluate the electromagnetic scattering characteristics. This approach has both advantages and disadvantages, which will be discussed in

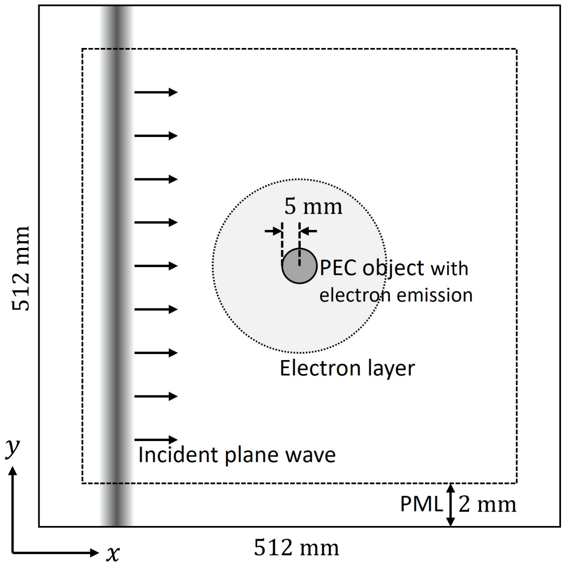

Fig. 2. Simulation configuration.

Table 1. Simulation parameters.

Items	Values
Maximum electron density	10^{11} /cc
Electron temperature	2 keV
Grid width	0.1 mm
Time step width	0.17 ps
System size	512^2 mm^2
Simulation time (1st phase)	1.7 ns
(2nd phase)	17 ns

Section **4.**.

Figure 2 shows the simulation configuration analyzed herein. The circular PEC object with a radius of 5 mm is placed in the center of the two-dimensional simulation domain with a side length of ∼ 0.5 m. This allows us to virtually consider radio waves scattered by a cylindrical conductor in three dimensions. The outer edges of the simulation domain are terminated by standard perfect matching layers (PML) against a free-space impedance. The layers can absorb outgoing waves because the electron density near the outer boundaries of the simulation is supposed to be very low. The spatial grid and the temporal step widths are set to 0.1 mm and 0.17 ps, respectively, in the simulations.

Thermal electrons are kept emitted from the PEC surface of the object throughout both phases of the simulation analysis. The current density and temperature of the emitted electrons are preset so that the density and temperature of the resulting electron population would be ∼ 10^{11} /cc and 2 keV, respectively. The parameters are also chosen to produce an electron layer thickness being in the order of mm. Based on these parameters, EMSES determines the number of electrons emitted within one simulation step as well as the initial velocities of the electrons. The initial positions are randomly distributed in azimuth on the cylindrical surface.

The numerical experiments are performed in the absence of a static magnetic field. Since we employ a dense local plasma, its electron cyclotron frequency is significantly lower than the local plasma frequency, even if we assume a geomagnetic field in the Earth's ionosphere. In this situation, the electron gyroradii

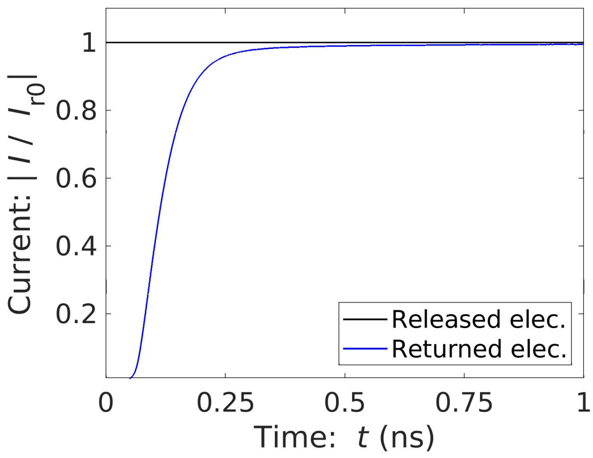

Fig. 3. Time history of electric current magnitudes carried by released and recollected electrons.

should be much greater than the electron layer thickness, and thus the magnetic field would have no appreciable impact on the electron dynamics within the layer. Also, the present analysis focuses only on the wave scattering by an electron population, and ignores any effects of ions. This is justified by the fact that ions, which are heavier than electrons, could not respond to high-frequency incident waves due to their greater inertia. If one were to focus on the scattering properties for lower frequency incident waves, ion dynamics would also be important. This aspect is, however, beyond the scope of the present study.

3.2. Electron layer formation

The first simulation phase is dedicated to the construction of a stable electron layer without applying any incident waves. We run a simulation until the time, in which a steady-state density profile is obtained. The total simulation time is 1.7 ns. A time history of the electric current magnitudes carried by released and recollected electrons is shown in Fig. 3. In contrast to a constant rate of electron emission, an increasing number of electrons are recollected by the object. The electron emission leaves positive electric charges on the surface of the object. The object attaining a positive potential exerts an attractive force on the surrounding electrons, which enhances the number of electrons that are attracted back to and recollected by the object. In the final stage, 99.6% of the emitted electrons are recollected by the object, and the remainder is accounted for by the high-energy fraction of the Maxwellian electrons escaping from the simulation domain. This confirms the completion of a steady-state electron layer formation.

Figure 4 shows the two-dimensional profiles of electron volume density and electric potential obtained at the last stage of the first simulation phase. Reflecting the axisymmetric nature of the simulation configuration, both density and potential profiles exhibit concentric structures. The electron density reaches its maximum value of 1.6×10^{11} /cc just outside the cylindrical body and decays sharply with distance from the body surface. The electric potential also has its maximum value within the cross section of the cylindrical body. It also decays with distance from the surface, but at a moderate rate compared to that of the electron density. This potential well contributes to the confinement of emitted electrons within the near-field region of the charged object. The different decay rates between

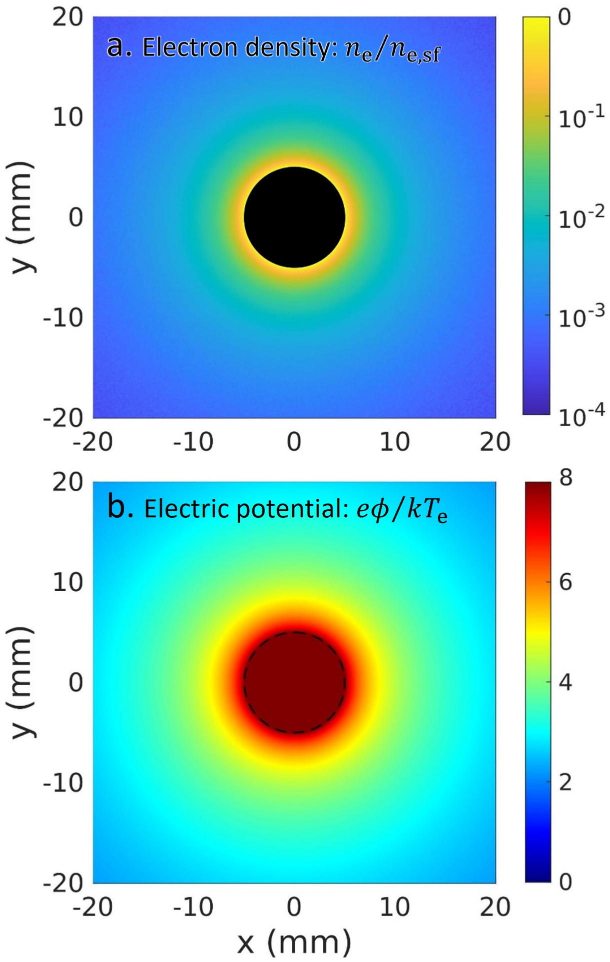

Fig. 4. Two-dimensional profiles of (a) electron volume density and (b) electric potential at the final stage of the first simulation. The centered circle represents the volume occupied by the object.

density and potential are attributed to the energy distribution of the thermal (i.e., Maxwellian) electrons. The fraction of thermal electrons with kinetic energies greater than ϵ scales as $\exp((-\epsilon)/(kT_e))$. It follows that the density also decays as $n_e \sim n_{e,sf} \exp(e(\phi - \phi_{PEC})/(kT_e))$. In the state of dynamic equilibrium, the force balance is established between an inward electrostatic force and an outward pressure gradient force, the latter arising in the non-uniform electron population.

3.3. Radio wave scattering

The electron distribution outlined above is taken over by the second simulation phase, in which EMSES applies an incident plane electromagnetic wave propagating in the $+x$ direction. We focus on the wave scattered by the cylindrical object covered by the non-uniform, self-consistently produced electron layer. The incident wave has the waveform of a single Gaussian pulse along the x axis and is suitable for studying the broadband properties of electromagnetic scattering. We assume a linear polarization of the incident wave. Its electric field E^i and magnetic field B^i are aligned with y and z directions, respectively. The total simulation time of the second simulation phase is 17 ns. The duration is chosen to cover the converged responses of the low-frequency wave components.

Figure 5 displays the spatial profiles of the B_z components of the waves scattered by the PEC object (B_z^{so}) and the elec-

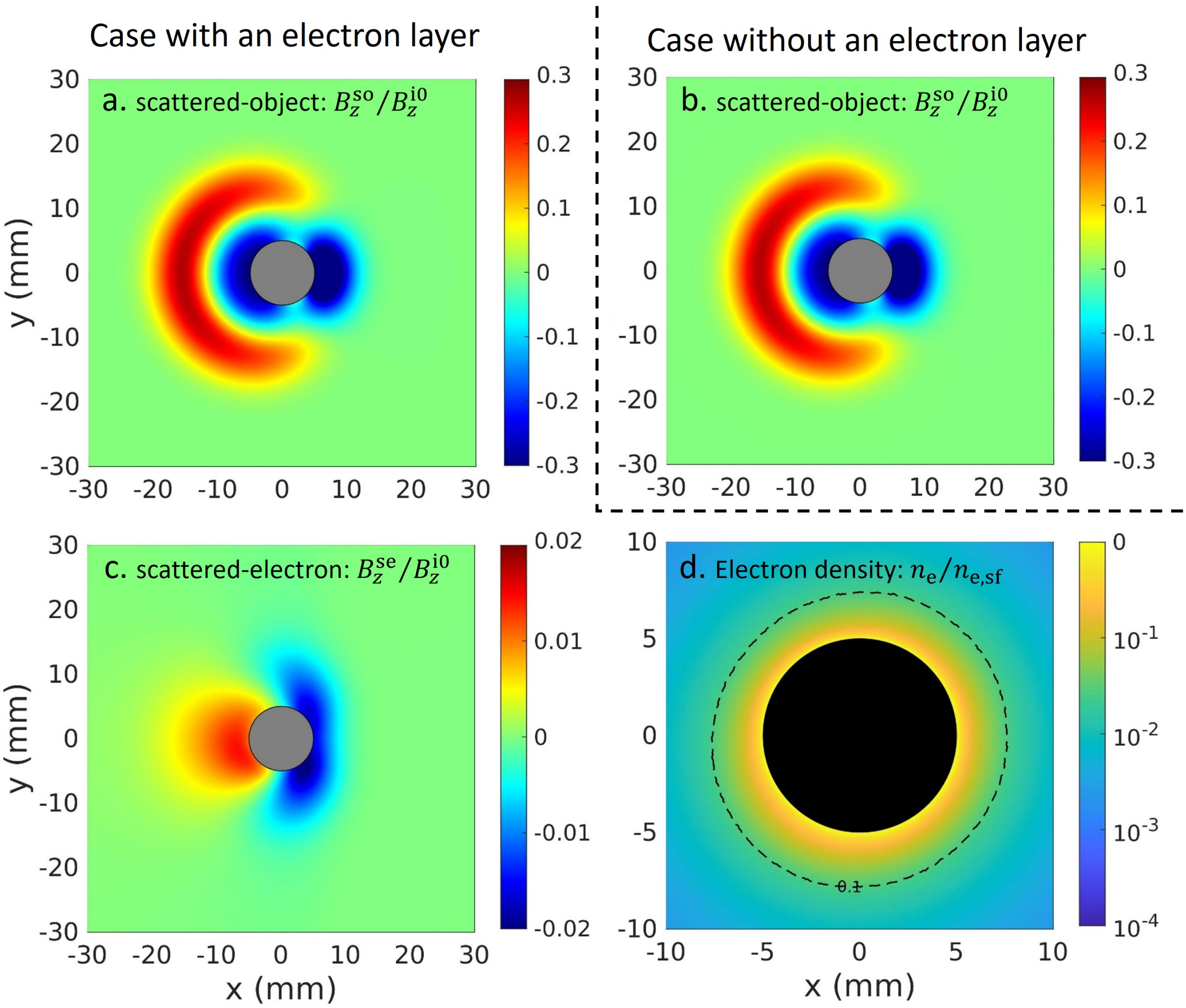

Fig. 5. Two-dimensional profiles of (a) the magnetic field component B_z^{so} of the waves scattered by the object, (b) the magnetic field component B_z^{so} of the waves scattered by the object, not covered by an electron layer, (c) the magnetic field component B_z^{se} of the waves scattered by the electron layer, and (d) the electron volume density, at t = 0.033 ns after the impact of the incident wave pulse. The magnetic field values are normalized to the field amplitude B_z^{i0} of the incident wave.

tron population (B_z^{se}) at 0.033 ns after the impact of the incident wave pulse. For reference, we also show a result obtained from a separate simulation without any electron emission (Fig. 5b). Note that we use different color scales between B_z^{so} and B_z^{se} for visibility. As for the B_z^{so}, the result with the electron layer (Fig. 5a) is almost identical to the case without the layer (Fig. 5b). The reason for the appearance match would be that the intensity of the multiply scattered field is much smaller than that of the primary scattering. The clear signature of wave scattering is identified, which arises primarily at the PEC surface of the object. This is evident from the fact that the B_z^{so} profile is almost identical to that computed without an electron layer, which is non-trivial as B_z^{so} potentially contains a multiply scattered component between the object surface and the surrounding electrons. Although the Gaussian-shaped incident wave has a broadband spectrum, its pulse width in use is comparable to the object radius. Thus, the features of the Rayleigh and Mie scattering[25] are identifiable in the resulting pattern of B_z^{so}.

The simulation also reveals the structure of a scattered field B_z^{se} caused by an electron layer. The field is much smaller in magnitude than B_z^{so}, and its spatial pattern is asymmetric between the backward ($-x$) and forward ($+x$) sides of the object. On the forward side, the scattered fields B_z^{se} and B_z^{so} mutually reinforce each other, implying an electron layer effect that enhances the forward scattering. The implication of an electron layer contribution to backward scattering is more complex, as B_z^{so} exhibits the sign-inverted field structure. We will revisit this aspect by showing the monostatic radar cross section (RCS) in a wavenumber domain.

The nature of the identified scattering process should be considered in terms of an electric current induced by electron motions affected by the incident wave. As the incident wave passes, its electric field E_y^i pushes the electron population within the wave envelope. The wave magnetic field is virtually irrelevant in the present small amplitude regime; the average gyroradius of the electrons is sufficiently greater than the spatial extent of the electron cloud. The consequence of altered electron motions is illustrated in an electron density profile at the moment of wave passage (Fig. 5d), which shows that an electron density structure is slightly shifted. It will be shown later that this displacement is associated with a downward motion of the electron layer at t = 0.033 ns. Since the electrons are anchored to the charged object by an electrostatic force of attraction, the electron population returns to its original position after the passage

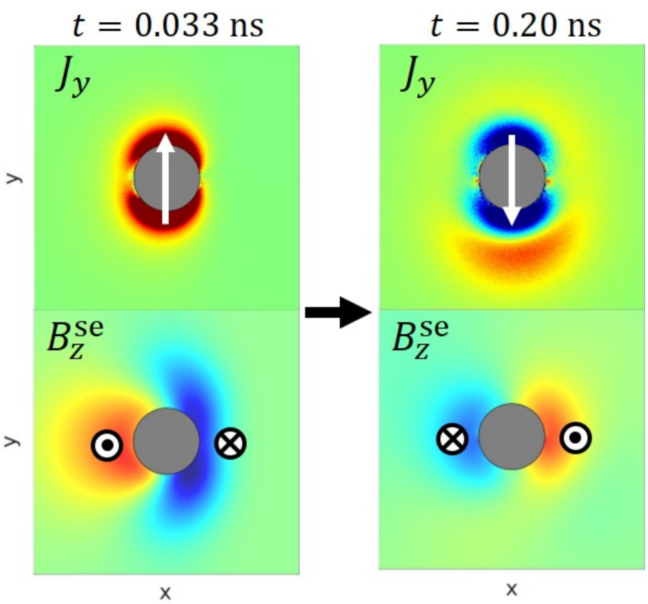

Fig. 6. The electron layer behavior analogous to a radiating dipole antenna. The electric current induced by the motion of the electron population is associated with the magnetic field component of the radiated wave . The white arrows in the upper panel represent the directions of the global current induced by the electron layer oscillation.

of the incident wave.

The outlined scattering process can be interpreted as the reradiation of electromagnetic waves from a moving electron population under the action of the incident wave. Figure 6 illustrates the relationship between an induced current within the electron population and the spatial profiles of the radiated waves. At $t = 0.033$ ns, the electron population undergoes a downward force from the incident wave, which produces a current $J_y > 0$ within the electron population. The small displacement of the electron layer as seen in Fig. 5d is the consequence of this downward motion. After the passage of the incident waves, e.g., at $t = 0.20$ ns, a reverse current $J_y < 0$ develops in association with the restoring motion of the electron population. At each phase, the opposed magnetic field in the z direction is produced on both sides of the current structure and radiated outward. This electron layer action, analogous to a dipole antenna, contributes to the alternation of the scattering properties of the core PEC object.

We close the section with the evaluation of a monostatic RCS σ_e for the object covered by the electron layer. The comparison of σ_e with the RCS σ_f without an electron layer is shown in Fig. 7. We use the total backscattered signal, i.e., $B^{so} + B^{se}$ for the computation, and thus the obtained RCS is relevant for radar observations of such objects. The effect of the electron layer can be summarized as follows: (1) In a low wavenumber range, the electron layer significantly enhances the RCS. (2) In the medium wavenumber range, the electron layer reduces the RCS. (3) In the high wavenumber range, the RCS of the electron-covered object converges to that of the electron-free object.

A number of discrepancies are identified in the present study with previous related works. The previous works mostly employed a uniform-density electron column model with a certain thickness12). The RCS in the low wavenumber limit was reported to be identical to that of the coalesced structure of the core conductor and the plasma column. This is in contrast to the situation and the result considered herein. This interesting aspect would be attributed to the widespread electron density profile. Electromagnetic waves propagating in a plasma of increasing density are reflected at a point with a so-called "critical density", which is an increasing function of the wave frequency. This implies that incident waves of different wavenumbers (i.e., frequencies) will be reflected or scattered at different positions.

Another feature of the present result is that the obtained RCS does not exhibit any resonance signature between the low and medium wavenumber regimes. Although such a resonant nature is referred to as being observed at the Tonks-Dattner resonant frequency,[26] it is difficult to identify such a specific frequency here due to the spatial variation of the electron density. Whatever the frequency (wavenumber) is, some sort of dissipation mechanism would be required to justify the non-resonant feature in the computed RCS. Although the present simulations do not include the effects of electron-neutral collisions, the conversion of electromagnetic energy into some form of electron kinetic energy can be cited as an alternative dissipative process. In addition, all the electrons simulated herein undergo repetitive emission and recollection processes at the surface of the solid object. Such process is regarded as one form of inelastic collisions. These processes can be identified as a potential dissipative factor. However, detailed investigations of this interesting aspect are beyond the scope of this paper, and will be elaborated in the future.

4. Discussions and Conclusions

We have proposed a new approach for the study of radio wave scattering by an object covered with a layer of charged particles. The proposed approach is based on the standard particle-in-cell method, but some additional dedicated functions, such as the field decomposition capability, are added for its application to the wave scattering problem. The developed code is applied to the two-dimensional computation simulating a rather simplified case where a cylindrical object is covered with an electron layer in an axisymmetric manner. The two separate simulation phases are devoted to the self-consistent formation of an electron density structure and the analysis of radio wave scattering for the target object. Despite the demonstration purpose, the simulation produces some interesting results exhibiting an antenna-like behavior of the electron layer swayed by an incident wave, and its contribution to the differentiated wave scattering properties.

In this study, the three-way interactions between a charged particle population, a conducting object, and electromagnetic waves have been taken as a case study for the application of the developed method. In principle, the developed approach would also be applicable to fundamental wave scattering processes emerging in the ionospheric environment, such as the interference between plasmas and neutrals. The implementation of a collision model between charged and neutral particles in the simulator and the numerical analysis based on it would be a good candidate for further benchmarking of the developed approach.

The proposed approach is distinguished from previous FDTD

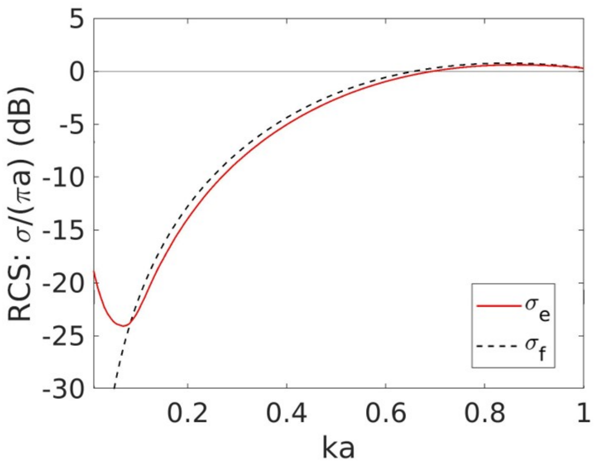

Fig. 7. Monostatic RCS profiles in a wavenumber domain for objects with and without an electron layer. The horizontal axis represents the wavenumber normalized using the object radius *a*.

simulations, which are based on the dielectric representation of a plasma, in the treatment of the charged particle distribution. The distribution is treated as a prescribed model in the previous study, whereas the PIC approach basically "reproduces" the distribution through self-consistent simulations of charged particle kinetics. Both approaches have their advantages and disadvantages. The present method can be free from a priori assumptions about the charge density distribution, but it also demonstrates the difficulty of employing arbitrary configurations of charged particle configurations as input parameters of the analysis. In addition, its high computational cost and numerical stability constraints often limit the applicability of the approach in parameter space, and the analysis demonstrated in this study actually assumes a very high electron density. This indicates that in practice, some scaling process is often necessary to adapt the obtained numerical results to the target problems. In summary, the combined use of these complementary approaches would be beneficial for a better understanding of the plasma-based wave scattering processes.

Acknowledgments

YM wishes to thank Hiroshi Nakashima for continuous advice on the development of high-performance numerical algorithms and the efficient use of supercomputers. The authors also thank Nobuyuki Kaya and Hideyuki Usui for fruitful discussions on the interpretation of the simulation results. The computations in this study were performed on the Cray XC40 at Kyoto University and the FUJITSU PRIMERGY CX1640 M1 at Hokkaido University. This research and development work was supported by the MIC/SCOPE #JP196000002.

References

1) Dolph, C. L. and Weil, H.: On the Change in Radar Cross-Section of a Spherical Satellite Caused by a Plasma Sheath, *Planet. Space Sci.*, **6** (1961), pp. 123–132.
2) Swarner, W. G. and Peters, L. Jr.: Radar Cross Sections of Dielectric or Plasma Coated Conducting Spheres and Circular Cylinders, *IEEE Trans. Antennas Propag.*, **11** (1963), pp. 558–569.
3) Singh, H., Antony, S., and Jha, R. M.: *Plasma-based Radar Cross Section Reduction*, Springer, Singapore, 2016.
4) Rybak, J. P. and Churchill, R. J.: Progress in Reentry Communications, *IEEE Trans. Aerospace. Electron. Syst.*, **5** (1971), pp. 879–894.
5) Zheng, L., Zhao, Q., and Xing, X. J.: Effect of Plasma on Electromagnetic Wave Propagation and THZ Communications for Reentry Flight, *Applied Comput. Electromagnetics Soc. J.*, **30** (2015), pp. 1241–1245.
6) Chen, H. C. and Cheng, D. K.: Scattering of Electromagnetic Waves by an Anisotropic Plasma-Coated Conducting Cylinder, *IEEE Trans. Antennas Propag.*, **12** (1964), 348–353.
7) Yin, B., F. Yang, H. Hao, and C. Li, Analysis of Scattering Wave for a Conducting Cylinder Coated with Eccentric Plasma, *Radiation Effects and Defects in Solids*, **168** (2013), pp. 344–351.
8) Laroussi, M. and Roth, J. R.: Numerical Calculation of the Reflection, Absorption, and Transmission of Microwaves by a Nonuniform Plasma Slab, *IEEE Trans. Plasma Sci.*, **21** (1993), pp. 366–372.
9) Hu, B. J., Wei, G., and Lai, S. L.: SMM Analysis of Reflection, Absorption, and Transmission from Nonuniform Magnetized Plasma Slab, *IEEE Trans. Plasma Sci.*, **27** (1999), pp. 1131–1136.
10) Chaudhury, B. and Chaturvedi, S.: 3-d Simulations for Radar Cross-Section Reduction using Plasma Absorbers, 33rd IEEE International Conference on Plasma Science, pp. 24–24, 2006.
11) Chaudhury, B. and Chaturvedi, S.: Study and Optimization of Plasma-Based Radar Cross Section Reduction Using Three-Dimensional Computations, *IEEE Trans. Plasma Sci.*, **37** (2009), pp. 2116–2127.
12) Naito, T., Tanaka, T., Fukuma, Y., and Sakai, O.: Electromagnetic Wave Cloaking and Scattering around an Antiresonance- Resonance Symmetrical Pair in the Frequency Domain, *Phys. Rev. E*, **99** (2019), p. 013204.
13) Lapenta, G.: Exactly Energy Conserving Semi-Implicit Particle in Cell Formulation, *J. Comput. Phys.*, **334** (2017), pp. 349–366,
14) Miyake, Y. and Usui, H.: New Electromagnetic Particle Simulation Code for the Analysis of Spacecraft-Plasma Interactions, *Phys. Plasmas*, **16** (2009), p. 062904.
15) Dawson, J. M.: Particle Simulation of Plasmas, *Rev. Mod. Phys.*, **55** (1983), pp. 403–447.
16) Birdsall, C. K. and Langdon, A. B.: Plasma Physics Via Computer, McGraw-Hill, Inc., 1985.
17) Hockney, R. W. and Eastwood, J. W.: Computer Simulation Using Particles, Taylor & Francis, Inc., 1981.
18) Boris, J. P.: Relativistic Plasma Simulation-Optimization of a Hybrid Code, Proc. 4th Conf. Num. Sim. Plasmas, pp. 3–67, 1970.
19) Taflove, A. and Hagness, S. C.: *Computational Electrodynamics: The Finite-Difference Time-Domain Method*, 2nd ed., Artech House, Norwood, Mass, 2000.
20) Taflove, A. and Brodwin, M. E.: Numerical Solution of Steady-State Electromagnetic Scattering Problems using the Three-Dependent Maxwell's Equations, *IEEE Trans. Microwave Theory Tech.*, **MTT-23** (1975), pp. 623–630.
21) Yee, K. S.: Numerical Solution of Initial Boundary Value Problems Involving Maxwell's Equations in Isotropic Media, *IEEE Trans. Antennas and Propag.*, **14** (1966), pp. 302–307.
22) Muranaka, T., Hosoda, S., Kim, J.-H., Hatta, S., Ikeda, K., Hamanaga, T., Cho, M., Usui, H., Ueda, H. O., Koga, K., and Goka, T.: Development of Multi-Utility Spacecraft Charging Analysis Tool (MUSCAT), *IEEE Trans. Plasma Sci.*, **36** (2008), pp. 2336–2349.
23) Nakashima, H., Miyake, Y., Omura, Y., and Usui, H.: OhHelp: A Scalable Domain-Decomposing Dynamic Load Balancing for Particle-in-Cell Simulations, Proc. of the 23rd Intl. Conf. on Supercomputing, pp. 90–99, 2009.
24) Miyake, Y. and Nakashima, H.: Low-cost Load Balancing for Parallel Particle-In-Cell Simulations with Thick Overlapping Layers, Intl. Symp. Parallel and Distributed Processing with Applications, pp. 1107–1114, 2013.
25) Stratton, J. A.: *Electromagnetic Theory*, New York: McGraw-Hill, 1941.
26) Dattner, A.: Resonance Densities in a Cylindrical Plasma Column, *Phys. Rev. Lett.*, **10** (1963), p. 205.